

## Synthesis, Thermal and Magnetic Properties of New Coordination Compounds based on $\text{Mn}(\text{NCS})_2$ with 2-Chloropyrazine and 2-Methylpyrazine as neutral Co-Ligand

Susanne Wöhlert,<sup>[a]</sup> Tomče Runčevski,<sup>[b]</sup> Robert E. Dinnebier,<sup>[b]</sup> and Christian Näther\*<sup>[a]</sup>

**Keywords:** Crystal structures; Thiocyanato coordination compounds; Thermal properties; Magnetic properties; Manganese

**Abstract.** Reaction of manganese(II) thiocyanate with 2-chloropyrazine leads always to the formation of a compound of composition  $\text{Mn}(\text{NCS})_2(2\text{-chloropyrazine})_4$  (**1-Mn/Cl**) that consists of discrete complexes, in which the manganese cation is coordinated by two terminal thiocyanato anions and four 2-chloropyrazine ligands. In contrast, with 2-methylpyrazine only an aqua complex of composition  $\text{Mn}(\text{NCS})_2(2\text{-methylpyrazine})_2(\text{H}_2\text{O})_2$  (**1-Mn/CH<sub>3</sub>**) is obtained that also consists of discrete octahedrally coordinated complexes. Moreover, a few single crystals of  $\text{Mn}(\text{NCS})_2(2\text{-chloropyrazine})_4$ ,  $\text{Mn}(\text{NCS})_2(2\text{-chloropyrazine})_2(\text{H}_2\text{O})_2$ -2-chloropyrazine trisolvate (**2-Mn/Cl**) and  $\text{Mn}(\text{NCS})_2(2\text{-methylpyrazine})_2(\text{H}_2\text{O})_2 \cdot \text{Mn}(\text{NCS})_2(\text{H}_2\text{O})_4$  (**2-Mn/CH<sub>3</sub>**) were accidentally obtained but no larger amounts are available. On heating, **1-Mn/Cl** and **1-Mn/CH<sub>3</sub>** transforms into new compounds of composition  $\text{Mn}(\text{NCS})_2(\text{L})_2$  ( $\text{L} = 2\text{-chloropyrazine}$ ) (**4-Mn/Cl**) and 2-methylpyrazine (**3-Mn/CH<sub>3</sub>**). Surprisingly on further heating

**1-Mn/CH<sub>3</sub>** loses additional 2-methylpyrazine ligands and transforms into a new compound of composition  $\text{Mn}(\text{NCS})_2(2\text{-methylpyrazine})$  (**4-Mn/CH<sub>3</sub>**). Compound **4-Mn/Cl** is isotypic to its cobalt(II) analog and **4-Mn/CH<sub>3</sub>** is isotypic to  $\text{Cd}(\text{NCS})_2(2\text{-methylpyrazine})$  reported recently and therefore, both structures were refined by the Rietveld method. The crystal structures of both compounds are strongly related. They consist of dimeric units, in which each two manganese cations are linked by pairs of  $\mu$ -1,3-bridging thiocyanato anions, which are further connected into layers by single  $\mu$ -1,3-bridging anionic ligands. In contrast to **4-Mn/Cl**, in **4-Mn/CH<sub>3</sub>** these layers are further linked into a 3D coordination network by the 2-methylpyrazine ligands. Magnetic measurements reveal that **1-Mn/Cl**, **1-Mn/CH<sub>3</sub>**, and **3-Mn/CH<sub>3</sub>** shows only Curie- or Curie-Weiss paramagnetism, whereas **4-Mn/Cl** and **4-Mn/CH<sub>3</sub>** shows antiferromagnetic ordering at  $T_N = 22.9$  K and at 26.5 K. The results of these investigations are compared with those obtained for related compounds.

### Introduction

Investigations on the synthesis, structures, and magnetic properties of new coordination compounds make an important field in coordination chemistry<sup>[1–7]</sup> and studies on the correlation between the composition and the structures of such compounds and their magnetic properties are of special interest.<sup>[8–13]</sup>

In this context, thio- and selenocyanato coordination compounds are of special interest because of the dependency of the magnetic behavior on the coordination mode and the nature of the metal cations, e.g. cooperative magnetic phenomena and spin crossover.<sup>[14–25]</sup>

In the focus of our research are the magnetic properties of transition metal thio- or selenocyanato coordination compounds based on Mn, Fe, Co, and Ni and different N-donor

ligands, in which the metal cations are linked by bridging anionic ligands.<sup>[26–31]</sup> Some of those compounds can be prepared in solution, other, however, are accessible only by thermal decomposition of suitable precursor compounds.<sup>[32,33]</sup> The synthesis of coordination compounds by classical solid state methods is not unusual and different methods are reported in literature.<sup>[34–37]</sup> In the course of our investigations, several new compounds were prepared, some of them showing a slow relaxation of the magnetization.<sup>[38–42]</sup> Such compounds are of special importance because of the potential for future practical applications.<sup>[43–47]</sup> Following our approach, 1D and 2D compounds can be selectively prepared by using mono- or bidentate N-donor co-ligands, which allows to study the influence of the structure on the magnetic properties in more detail.

Recently we reported new coordination polymers based on  $\text{Mn}(\text{NCS})_2$  and pyridine, 1,2-bis(4-pyridyl)-ethylene (4-bpe) and 1,2-bis(4-pyridyl)-ethane (4-bpa).<sup>[48–50]</sup> In these structures the metal cations are linked by pairs of  $\mu$ -1,3-bridging thiocyanato anions forming chains, which unlike in the case of the pyridine compound, are connected into layers. Magnetic measurements reveal that for all of the compounds antiferromagnetic ordering is observed. To study the influence of the topology of the thiocyanato network on the magnetic properties in more detail, we tried to prepare the corresponding compounds with 2-chloro- and 2-methylpyrazine as neutral co-li-

\* Prof. Dr. C. Näther  
Fax: +49-431-8801520  
E-Mail: cnaether@ac.uni-kiel.de

[a] Institut für Anorganische Chemie  
Christian-Albrechts-Universität zu Kiel  
Max-Eyth-Straße 2  
24118 Kiel, Germany

[b] Max-Planck-Institute for Solid State Research  
Heisenbergstraße 2  
70569 Stuttgart, Germany

Supporting information for this article is available on the WWW under <http://dx.doi.org/10.1002/zaac.201300361> or from the author.

gands. It should be noted that in the structures of similar compounds based on  $\text{Fe}^{\text{II}}$ ,  $\text{Co}^{\text{II}}$ , and  $\text{Ni}^{\text{II}}$  thiocyanates, surprisingly, instead of linear chains, a 2D thiocyanato network is formed, a very rare and unusual observation.<sup>[51–54]</sup> In this context, the question arises whether  $\text{Mn}(\text{NCS})_2$  will form similar 2D network with these ligands and how this will influence the magnetic properties of these compounds. Herein we report on these investigations.

## Results and Discussion

### Synthesis

At the beginning of our investigations, different molar ratios of  $\text{Mn}(\text{NCS})_2$  and 2-chloropyrazine or 2-methylpyrazine (1:4, 1:2, 1:1, 2:1, 4:1) were stirred in water, methanol, ethanol, and acetonitrile at room-temperature and the products were investigated by X-ray powder diffraction. Independent on the actual stoichiometry and the solvent used in the synthesis, only one compound with 2-chloropyrazine (**1-Mn/Cl**) and one with 2-methylpyrazine (**1-Mn/CH<sub>3</sub>**) were obtained. The structures of these compounds were found not to be isotopic. Elemental analysis reveal that the composition of **1-Mn/Cl** is  $\text{Mn}(\text{NCS})_2(2\text{-chloropyrazine})_4$  and that the ratio between  $\text{Mn}(\text{NCS})_2$  and 2-methylpyrazine is 1:2:2 in **1-Mn/CH<sub>3</sub>**. The asymmetric CN stretching vibration observed in the IR spectrum was found at  $2067\text{ cm}^{-1}$  for **1-Mn/Cl** and at  $2079\text{ cm}^{-1}$  for **1-Mn/CH<sub>3</sub>** indicating that only terminal N-bonded thiocyanato anions are present (see Figures S1 and S2, Supporting Information). From these investigations there are no hints for the occurrence of additional compounds, in which the manganese cations are linked by bridging thiocyanato anions.

Single crystals of both compounds were prepared and characterized by single-crystal X-ray analysis. The bulk material of **1-Mn/CH<sub>3</sub>** was shown to be phase pure (Figure S3, Supporting Information). However, some of the powder patterns of **1-Mn/Cl** showed additional reflections, especially if stored at ambient conditions, indicating the presence of an additional crystalline phase, which gains in amount when **1-Mn/Cl** is exposed to the atmosphere. By storing the powder for a longer period of time it transforms completely into a hydrate phase (**3-Mn/Cl**) with an approximate composition of  $\text{Mn}(\text{NCS})_2(2\text{-chloropyrazine})_2(\text{H}_2\text{O})_x$ . The trials for solving the crystal structure, so far, did not result in solution, however, the phase was indexed in a monoclinic unit cell (space group  $P2_1/c$ ) and  $a = 16.879(5)\text{ \AA}$ ,  $b = 9.854(3)\text{ \AA}$ ,  $c = 15.039(6)\text{ \AA}$ ,  $\beta = 83.53(1)^\circ$  (see Figure S4, Supporting Information). IR investigations shows two bands at  $2064\text{ cm}^{-1}$  and  $2082\text{ cm}^{-1}$  indicating that only terminal coordinated thiocyanato anions are present (see Figure S5, Supporting Information). Moreover, a broad band is observed in the region between  $3000$  and  $3500\text{ cm}^{-1}$  indicating that water is present.

Within these investigations, crystals of two further compounds of composition  $\text{Mn}(\text{NCS})_2(2\text{-chloropyrazine})_4$ ,  $\text{Mn}(\text{NCS})_2(2\text{-chloropyrazine})_2(\text{H}_2\text{O})_2 \cdot 2\text{-chloropyrazine}$  tri-solvate (**2-Mn/Cl**) and  $\text{Mn}(\text{NCS})_2(2\text{-methylpyrazine})_2(\text{H}_2\text{O})_2 \cdot \text{Mn}(\text{NCS})_2(\text{H}_2\text{O})_4$  (**2-Mn/CH<sub>3</sub>**) were obtained by accident.

### Crystal Structures of **1-Mn/Cl**, **1-Mn/CH<sub>3</sub>**, **2-Mn/Cl**, and **2-Mn/CH<sub>3</sub>**

The compound **1-Mn/Cl** crystallizes in the monoclinic space group  $P2_1/n$  with two formula units in the unit cell. The asymmetric unit consists of one manganese(II) cation located on a center of inversion and one thiocyanato anion as well as two 2-chloropyrazine ligands in general positions. Each cation is coordinated by two terminal N-bonded thiocyanato anions and four N-bonded neutral co-ligands into discrete complexes (Figure 1 left). It should be noted that only the nitrogen atom of the co-ligand that is not adjacent to the bulky chlorine substituent is involved in metal coordination. The  $\text{MnN}_6$  distances are in the range of  $2.144(3)\text{ \AA}$  to  $2.345(3)\text{ \AA}$  with angles around the manganese(II) cation of  $87.24(9)^\circ$  to  $92.76(9)^\circ$  and  $180^\circ$  (see Table S1, Supporting Information).

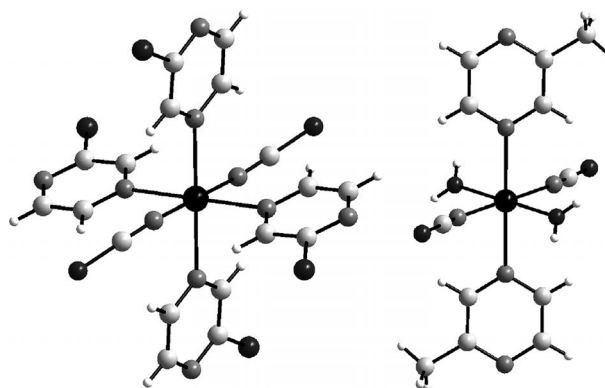


**Figure 1.** View of the coordination spheres in **1-Mn/Cl** (left) and **1-Mn/CH<sub>3</sub>** (right; black = manganese, dark-grey = sulfur / chlorine, grey = nitrogen, light-grey = carbon, white = hydrogen). ORTEP plots of both compounds can be found in Figures S6 and S7 (Supporting Information).

The compound **1-Mn/CH<sub>3</sub>** crystallizes in the triclinic space group  $P\bar{1}$  with one formula in the asymmetric unit. One manganese(II) cation is located on a center of inversion, whether the thiocyanato anions, the 2-methylpyrazine ligand, and the water molecule are on a general position. In the crystal structure each manganese(II) cation is coordinated by two terminal N-bonded thiocyanato anions and two 2-methylpyrazine ligands as well as two O-bonded water molecules (Figure 1 right). The  $\text{MnN}_4\text{O}_2$  octahedra are slightly distorted with distances in the range of  $2.172(2)\text{ \AA}$  to  $2.3131(17)\text{ \AA}$  and angles around the metal(II) cation ranging from  $88.14(9)^\circ$  to  $91.86(9)^\circ$  and  $180^\circ$  (see Table S2, Supporting Information). The discrete complexes are connected through intermolecular  $\text{OH}\cdots\text{S}$  hydrogen bonding [ $3.2607(19)\text{ \AA}$ ] into chains, which are elongate in the direction of the crystallographic  $a$  axis. These chains are further connected into layers through intermolecular  $\text{OH}\cdots\text{N}(2\text{-methylpyrazine})$  hydrogen bonding [ $2.8223(2)\text{ \AA}$ ] (see Figure S8, Supporting Information).

The compound **2-Mn/Cl** crystallizes in the triclinic space group  $P\bar{1}$  with one formula unit in the unit cell. The asymmetric unit consists of two crystallographically independent manganese(II) cations located on centers of inversion. One metal(II) cation is coordinated by two terminal N-bonded

thiocyanato anions, and four 2-chloropyrazine ligands and the second metal(II) cation is coordinated by two terminal N-bonded thiocyanato anions, two 2-chloropyrazine ligands, and two water molecules (see Figure S9, Supporting Information). The  $\text{Mn}_2\text{N}_{10}\text{O}_2$  octahedra are slightly distorted with distances ranging from 2.131(2) Å to 2.370(2) Å and angles around the manganese(II) cations in the range of 87.98(7)° to 92.02(7)°, and of 180° (see Table S3, Supporting Information). In the crystal structure cavities are found between the discrete complexes, in which additional non-coordinating 2-chloropyrazine ligands are present. One of these ligands is on a general position, whereas the second is disordered on a center of inversion. The discrete complexes are connected through intermolecular O–H···N hydrogen bonding [2.808(3) Å and 2.884(3) Å] into a 3D coordination network.

The compound **2-Mn/CH<sub>3</sub>** crystallizes in the tetragonal space group  $P4_3$  with four formula units in the unit cell. The asymmetric unit consists of two crystallographically independent manganese(II) cations, one coordinated by two terminal N-bonded thiocyanato anions, two 2-methylpyrazine ligands, and two O-bonded water molecules and the second one coordinated by two terminal N-bonded thiocyanato anions and four O-bonded water molecules (Figure 2). All atoms are located on a general position. The  $\text{Mn}_2\text{N}_6\text{O}_6$  octahedra are slightly distorted with distances ranging from 2.153(3) Å to 2.296(3) Å and angles around the manganese(II) cations in the range of 85.06(11)° to 94.57(12)° and 177.19(15)° to 178.34(11)° (see Table S4, Supporting Information). In the crystal structure the manganese(II) octahedra are connected through intermolecular hydrogen bonding into a 3D coordination network (see Table S5, Supporting Information).

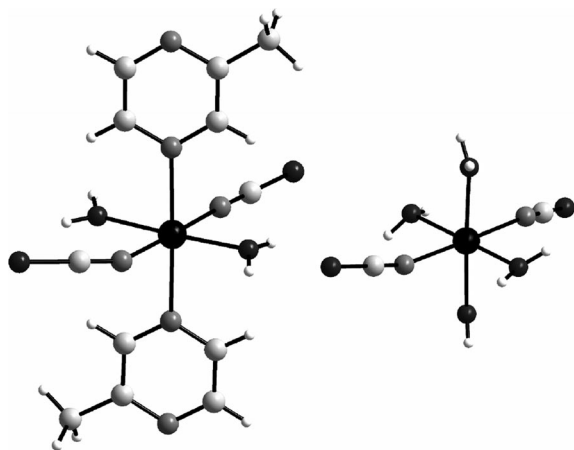


**Figure 2.** View of the coordination sphere in **2-Mn/CH<sub>3</sub>** (black = manganese, dark-grey = sulfur / oxygen, grey = nitrogen, light-grey = carbon, white = hydrogen). An ORTEP plot can be found in Figure S10 (Supporting Information).

### Thermoanalytical Investigations

In order to investigate whether the compounds with  $\mu$ -1,3-bridging thiocyanato anions can be obtained by thermal decomposition of **1-Mn/Cl** and **1-Mn/CH<sub>3</sub>** both of them were

studied by simultaneous thermogravimetry and differential thermoanalysis. On heating to 300 °C two mass loss steps are observed for **1-Mn/Cl** and three for **1-Mn/CH<sub>3</sub>**, accompanied with respective endothermic events in the DTA curve (Figure 3).

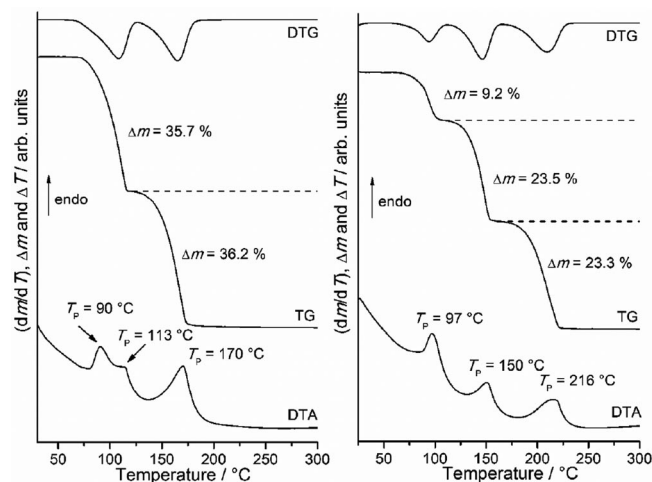


**Figure 3.** DTG, TG, and DTA curves for **1-Mn/Cl** (left) and **1-Mn/CH<sub>3</sub>** (right). Heating rate 4 K·min<sup>-1</sup>, N<sub>2</sub> atmosphere, Al<sub>2</sub>O<sub>3</sub> crucible,  $\Delta m$  = mass loss /%,  $T_p$  = peak temperature /°C.

The experimental mass loss of  $\Delta m_{\text{exp}} = 35.7\%$  in the first and  $\Delta m_{\text{exp}} = 36.2\%$  in the second step of **1-Mn/Cl** are in agreement with that calculated for the removal of two 2-chloropyrazine ligands in each step ( $\Delta m_{\text{calc}} = 36.4\%$ ). These results indicate that in the first heating step a compound of composition  $\text{Mn}(\text{NCS})_2(2\text{-chloropyrazine})_2$  (**4-Mn/Cl**) is formed, which decomposes into manganese thiocyanate in the second step. The experimental mass loss of  $\Delta m_{\text{exp}} = 9.2\%$  for **1-Mn/CH<sub>3</sub>** is in agreement with that calculated for the removal of two water molecules in the first heating step ( $\Delta m_{\text{calc}} = 9.11\%$ ). These results indicate that in the first TG step a new 1:2 compound of composition  $\text{Mn}(\text{NCS})_2(2\text{-methylpyrazine})_2$  (**3-Mn/CH<sub>3</sub>**) is formed. The experimental mass loss of  $\Delta m_{\text{exp}} = 23.5\%$  in the second step is in very good agreement with the loss of one 2-methylpyrazine ( $\Delta m_{\text{calc}} = 23.8\%$ ). Therefore it can be assumed that the intermediate **3-Mn/CH<sub>3</sub>** transforms into a new 1:1 compound of composition  $\text{Mn}(\text{NCS})_2(2\text{-methylpyrazine})$  (**4-Mn/CH<sub>3</sub>**) whether on further heating that decomposes into manganese(II) thiocyanate.

Similar investigations on the hydrate **3-Mn/Cl** show that on heating water is removed leading to the formation of a compound of composition  $\text{Mn}(\text{NCS})_2(2\text{-chloropyrazine})_2$  (**4-Mn/Cl**) (see Figure S11, Supporting Information).

To verify the nature of the intermediate additional TG experiments were performed and stopped after the first and second TG step and the obtained residues were investigated by elemental analysis and IR spectroscopy (see Figures S12–S14, Supporting Information). For the 2-chloropyrazine compound **4-Mn/Cl** the asymmetric CN stretching vibration is observed at 2095 cm<sup>-1</sup> indicative for  $\mu$ -1,3-bridging thiocyanato anions. Surprisingly for the 2-methylpyrazine-deficient compound **3-Mn/CH<sub>3</sub>** that exhibit the same stoichiometry as **4-Mn/Cl** two

bands at  $2049\text{ cm}^{-1}$  and  $2034\text{ cm}^{-1}$  are observed, which strongly indicates that only terminal N-bonded thiocyanato anions are present. Finally, for  $4\text{-Mn}/\text{CH}_3$   $\nu_{\text{as}}(\text{CN})$  is observed at  $2099\text{ cm}^{-1}$ , which is characteristic for  $\mu$ -1,3-bridging thiocyanato anions.

Compound  $4\text{-Mn}/\text{Cl}$  was obtained as microcrystalline powder with good level of crystallinity. Its crystal structure was found to be isotypic to the recently reported structure of  $\text{Co}(\text{NCS})_2(2\text{-chloropyrazine})_2$ .<sup>[52]</sup> A Rietveld refinement was performed and the final plot is given in Figure 4.

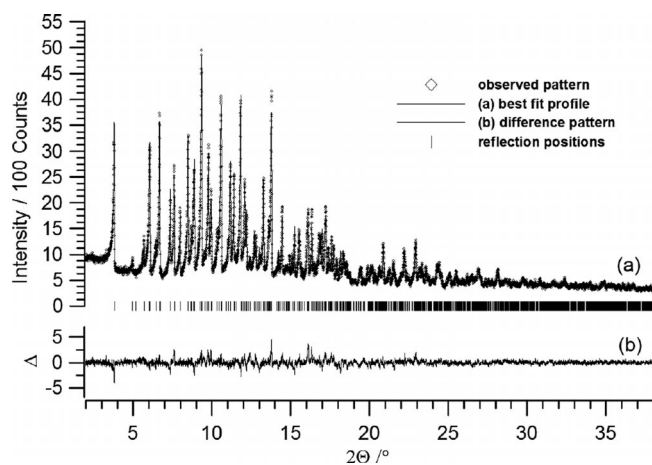


**Figure 4.** Scattered X-ray intensities of  $4\text{-Mn}/\text{Cl}$  as a function of diffraction angle at ambient conditions. The observed pattern (diamonds) measured in Debye-Scherrer geometry, the best Rietveld fit profile (line) and the difference curve between the observed and the calculated profiles (below) and the Bragg reflection positions are shown (wavelength =  $0.7093\text{ \AA}$ ).

The powder pattern of  $3\text{-Mn}/\text{CH}_3$  indicates that this compound has very low crystallinity; being characterized by few broad reflection (see Figure S15, Supporting Information). Interestingly, the powder pattern is very similar to that of  $M(\text{NCS})_2(2\text{-methylpyrazine})_2$  ( $M = \text{Fe}, \text{Co}$ ), indicating that the structures of these compounds are isotypic.<sup>[52]</sup> However, as in the case of the iron and the cobalt compounds, the powder pattern cannot be indexed and the structure of this intermediate remains to be unknown.

The next thermal product,  $4\text{-Mn}/\text{CH}_3$ , exhibits excellent crystallinity and its structure is isotypic to the reported structure of  $\text{Cd}(\text{NCS})_2(2\text{-methylpyrazine})$  (Figure 5).<sup>[51]</sup> In this context, it should be noted, that the formation of this intermediate with very low content of an N-donor ligand is quite unusual and was never observed before (mostly because metal cations like e.g. Mn, Fe, Co, and Ni are less chalcophilic and prefer only terminal bonding of the anionic ligands). In this case the formation of this compound is enforced by thermal decomposition and, as our results indicate, this compound cannot be obtained in solution. This is unlike similar compounds with cadmium because this metal cation is much more chalcophilic and therefore, such compounds are of extremely importance for the structure determination of their paramagnetic counterparts as shown recently.<sup>[55,56]</sup> The crystal structure of  $4\text{-Mn}/\text{CH}_3$  was refined using the Rietveld method and the final refinement plot is presented in Figure 5.

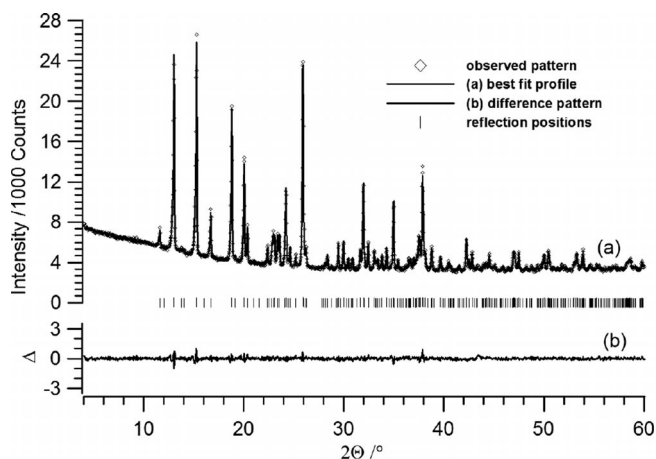


**Figure 5.** Scattered X-ray intensities of  $4\text{-Mn}/\text{CH}_3$  as a function of diffraction angle at ambient conditions. The observed pattern (diamonds) measured in Debye-Scherrer geometry, the best Rietveld fit profile (line) and the difference curve between the observed and the calculated profiles (below) and the Bragg reflection positions are shown (wavelength =  $1.540596\text{ \AA}$ ).

### Crystal Structures of $4\text{-Mn}/\text{Cl}$ and $4\text{-Mn}/\text{CH}_3$

As mentioned above,  $4\text{-Mn}/\text{Cl}$  is isotypic to its iron and cobalt analogs, whereas  $4\text{-Mn}/\text{CH}_3$  is isotypic to the corresponding cadmium compound.<sup>[51]</sup> Therefore, their crystal structures were refined by the Rietveld method (see Experimental Section). Because the structures of these compounds are already known only the most important features are summarized below. In both compounds the metal cations are octahedrally coordinated by two sulfur and two nitrogen atoms of thiocyanato anions, as well as by two nitrogen atoms of the N-donor ligands (Figure 6 and Figure S16, Supporting Information).

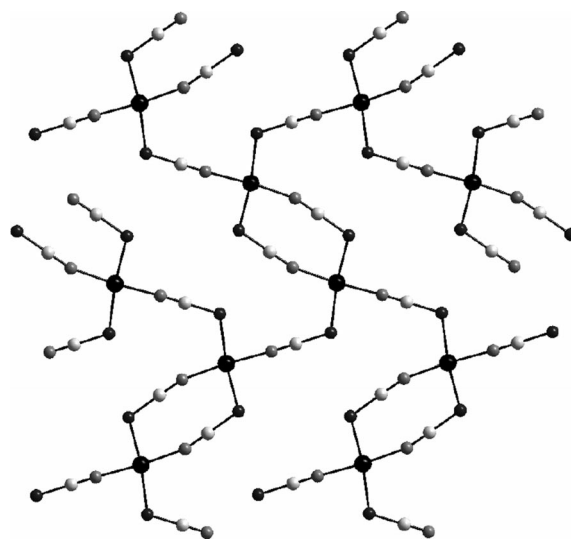


**Figure 6.** One layer of manganese(II) cations bridged by thiocyanato ligands in infinite chains in the crystal structures of  $4\text{-Mn}/\text{Cl}$  and  $4\text{-Mn}/\text{CH}_3$ . Please note that the N-donor co-ligands are omitted for clarity (black = manganese, dark-grey = sulfur, grey = nitrogen, light-grey = carbon).

Surprisingly, in both of them, an identical topology of the thiocyanato coordination network is observed. This topology is rather rare, and normally it is not observed in this type of coordination polymers. In the structures two manganese cations are linked by pairs of  $\mu$ -1,3-bridging thiocyanato anions into dimers, which are further linked by four single  $\mu$ -1,3-bridging anionic ligands, forming infinite layers.

In the structure of **4-Mn/Cl** the 2-chloropyrazine co-ligand is coordinated only by the nitrogen atom, which is not adjacent to the bulky chlorine atom. Therefore, this compound consists of a 2D coordination network (Figure 7 top). On the other hand, in the case of **4-Mn/CH<sub>3</sub>** the manganese thiocyanato layers are linked by bridging 2-methylpyrazine ligands into a 3D coordination network (Figure 7 bottom).

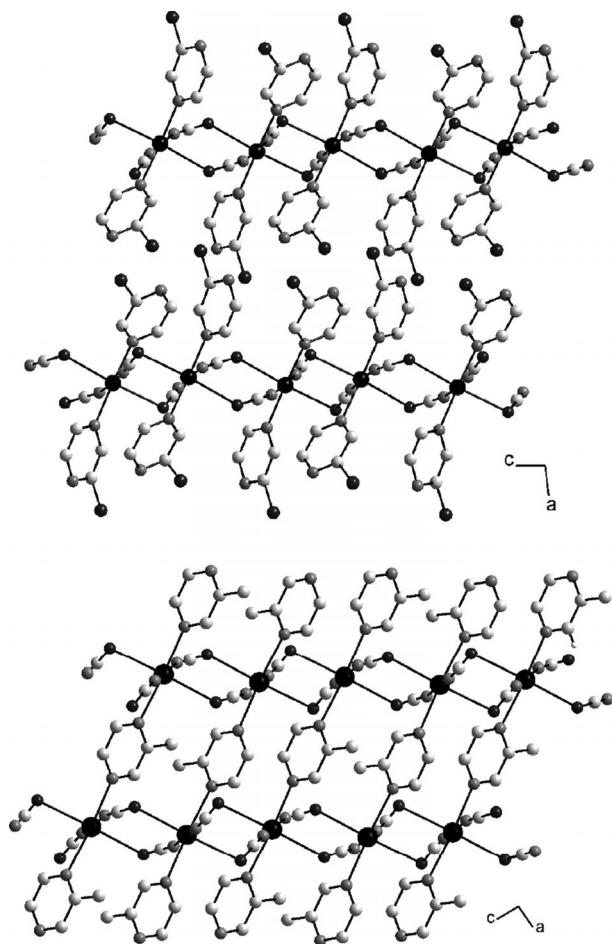


**Figure 7.** Crystal structure of **4-Mn/Cl** (top) and of **4-Mn/CH<sub>3</sub>** (bottom) with view along the crystallographic *b* axis (black = manganese, dark-grey = sulfur / chlorine, grey = nitrogen, light-grey = carbon).

### Magnetic Investigations

In order to investigate the magnetic properties of all compounds the temperature dependence of the susceptibility was studied applying a magnetic field of  $H_{DC} = 1$  kOe in the temperature range from 300 to 2 K. For the compounds **1-Mn/Cl**, **1-Mn/CH<sub>3</sub>**, and **3-Mn/CH<sub>3</sub>** only Curie or Curie-Weiss para-

magnetism is found (see Figure S17–S19, Supporting Information). The fitting of the magnetic curves following the Curie-Weiss law, gives Weiss constant of  $\theta = -0.80$  K for **1-Mn/Cl**,  $\theta = -0.02$  K for **1-Mn/CH<sub>3</sub>**, and  $\theta = -1.30$  K for **3-Mn/CH<sub>3</sub>**, which are very close to zero. The effective magnetic moments  $\mu_{eff}$  for **1-Mn/Cl** ( $5.97 \mu_B$ ), **1-Mn/CH<sub>3</sub>** ( $6.06 \mu_B$ ), and **3-Mn/CH<sub>3</sub>** ( $6.02 \mu_B$ ) are a bit higher than the spin-only value in the high-spin state of  $Mn^{2+}$  ( $S = 5/2$ ,  $g = 2$ ). These values are in agreement with the room-temperature values retrieved from the  $(8\chi_M T)^{1/2}$  vs. temperature curve, which also shows that in all compounds antiferromagnetic interactions are involved. In this context it is noted that the results obtained for **3-Mn/CH<sub>3</sub>** strongly support the results of the IR measurements and prove that in this compound only terminal N-bonded anionic ligands are present.

The magnetic measurements on **4-Mn/Cl** and **4-Mn/CH<sub>3</sub>** show maxima in the  $\chi_M$  vs.  $T$  curve at  $T_N = 22.9$  K for **4-Mn/Cl** and  $T_N = 26.5$  K for **4-Mn/CH<sub>3</sub>** indicative for antiferromagnetic ordering (Figure 8).

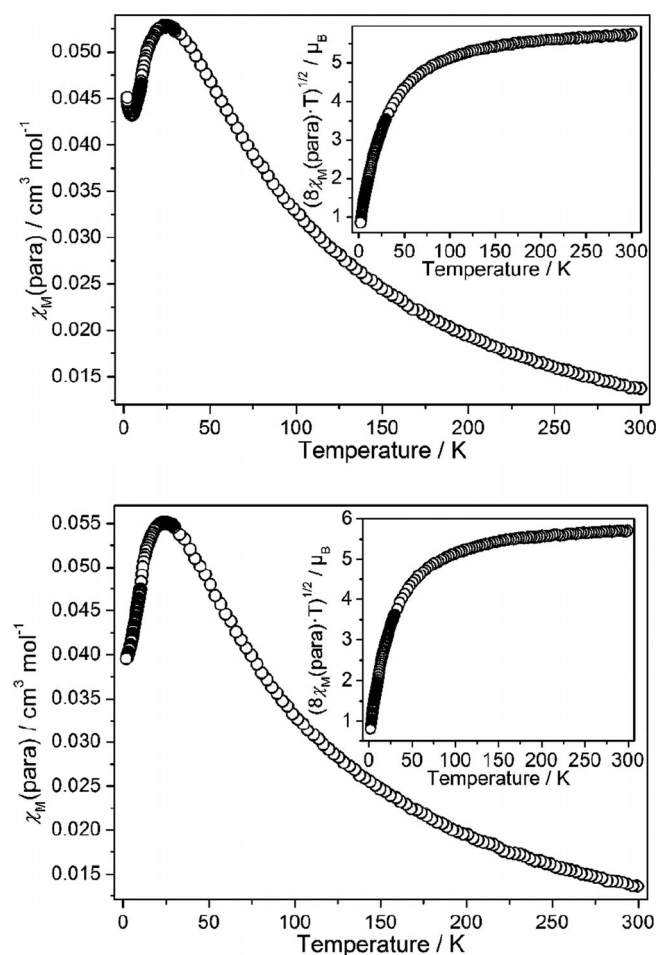


**Figure 8.**  $\chi_M$  and  $(8\chi_M T)^{1/2}$  (inset) as function of temperature for **4-Mn/Cl** (top) and **4-Mn/CH<sub>3</sub>** (bottom) at  $H_{DC} = 1$  kOe.

Fitting the magnetic data according to the Curie-Weiss law gives a strong negative Weiss constant of  $\theta = -45.8$  K for **4-Mn/Cl** and  $\theta = -41.2$  K for **4-Mn/CH<sub>3</sub>**, which is in agreement with the  $(8\chi_M T)^{1/2}$  vs. temperature curve that prove antiferro-

magnetic interactions. To exclude metamagnetic behavior an initial curve was measured for both compounds at  $T = 2$  K in the range of 0–9 kOe, which show linear increasing values typically for antiferromagnetic compounds (see Figures S20 and S21, Supporting Information).

It should be noted that in **4-Mn/Cl** the observed increase of the susceptibility at low temperatures might be a hint for canted antiferromagnetism or a paramagnetic impurity, which were not detected by X-ray powder diffraction. Therefore additional AC measurements were performed and no signal in the imaginary part ( $\chi_M''$ ) is observed, which means that spin-canting behavior can be excluded (see Figure S22, Supporting Information). In this context it is noted that a different batch that was stored for some time at room-temperature show only paramagnetic behavior (see Figure S23, Supporting Information). X-ray powder diffraction of this product proves that **4-Mn/Cl** is unstable at ambient conditions and transforms into the hydrate **3-Mn/Cl** (see Figure S24, Supporting Information).

As mentioned above, these investigations were performed in the scope of investigation of the magnetic properties of compounds of composition Mn(NCS)<sub>2</sub>(L)<sub>2</sub> with L being different co-ligands. The compounds with pyridine, 4-bpe, and 4-bpa consist of linear manganese thiocyanato chains and all of them show strong antiferromagnetic interactions and antiferromagnetic ordering on cooling.<sup>[48–50]</sup> Comparison of the magnetic data is given in Table 1.

**Table 1.** Comparison of selected magnetic data (at  $H_{DC} = 1$  kOe) for **4-Mn/Cl**, **4-Mn/CH<sub>3</sub>**, Mn(NCS)<sub>2</sub>(pyridine)<sub>2</sub>, Mn(NCS)<sub>2</sub>(pyridazine), Mn(NCS)<sub>2</sub>(4-bpe) [4-bpe = 1,2-bis(4-pyridyl)-ethylene] and Mn(NCS)<sub>2</sub>(4-bpa) [4-bpa = 1,2-bis(4-pyridyl)-ethane] retrieved from literature.<sup>[48–50]</sup>

	$T_N$ /K	$\theta$ /K
Mn(NCS) <sub>2</sub> (pyridine) <sub>2</sub>	23.5	–37.3
Mn(NCS) <sub>2</sub> (4-bpe)	26	–34.7
Mn(NCS) <sub>2</sub> (4-bpa)	24	–39.3
Mn(NCS) <sub>2</sub> (pyridazine)	14	–25.4
<b>4-Mn/Cl</b>	22.9	–45.8
<b>4-Mn/CH<sub>3</sub></b>	26.5	–41.2

Although the compounds with 2-methyl- and 2-chloropyrazine show a completely different topology of the thiocyanato coordination network, strong antiferromagnetic interactions and antiferromagnetic ordering is observed, which clearly proves that the magnetic properties of such compounds does not depend on the structure of the thiocyanato network, and it can be speculated that because of that antiferromagnetism is always observed for similar compounds. This is also indicated by the recently reported magnetic investigations on Mn(NCS)<sub>2</sub>(pyridazine).<sup>[57]</sup> Even though the structure of this compound is still unknown, the IR spectroscopic investigations clearly prove that the metal cations are linked by the thiocyanato ligands and magnetic measurements shows that this compound is an antiferromagnet.

## Conclusions

In the presented contribution, investigations on the synthesis, thermal and magnetic properties of manganese(II) thiocya-

nate coordination polymers based on 2-chloropyrazine and 2-methylpyrazine were reported. Two new compounds with  $\mu$ -1,3-bridging thiocyanato anions, which cannot be synthesized in solution, were prepared using the solid state route, showing the importance of thermal decomposition reactions for the preparation of compounds with more condensed thiocyanato networks.

Interestingly, the compounds with the bridging anionic ligands consist of a 2D thiocyanato network, which is not very common and which is completely different from that frequently found in compounds with similar co-ligands and identical ratio between Mn(NCS)<sub>2</sub> and the N-donor ligand. Surprisingly all of the compounds with  $\mu$ -1,3-bridging anions shows antiferromagnetic interactions and antiferromagnetic ordering, which proves that magnetic properties does not strongly depend on the composition of such compounds and of the topology of the thiocyanato coordination network.

## Experimental Section

**Materials:** MnSO<sub>4</sub>·2H<sub>2</sub>O, KNCS, 2-chloropyrazine, 2-methylpyrazine, and Ba(NCS)<sub>2</sub>·3H<sub>2</sub>O were obtained from Alfa Aesar and were used without further purification. Mn(NCS)<sub>2</sub> were prepared by the reaction of equimolar amounts of MnSO<sub>4</sub>·2H<sub>2</sub>O and Ba(NCS)<sub>2</sub>·3H<sub>2</sub>O in water. The resulting precipitate of BaSO<sub>4</sub> was filtered off and the filtrate was concentrated to complete dryness resulting in a white residue of Mn(NCS)<sub>2</sub>. The purity was checked by XRPD and elemental analysis. All crystalline powders were prepared by similar reaction conditions and stirring for 3 d. The obtained residues were filtered off and washed with water and diethyl ether and dried in vacuo. The purity was checked by XRPD and elemental analysis.

**Synthesis of 1-Mn/Cl:** Single crystals suitable for X-ray structure determination were obtained by the reaction of Mn(NCS)<sub>2</sub> (25.6 mg, 0.15 mmol) and 2-chloropyrazine (52.8  $\mu$ L, 0.6 mmol) in water (1 mL) in a closed snap cap vial. Yellow block-shaped single crystals were obtained after one week at room-temperature. Yield based on Mn(NCS)<sub>2</sub>: 163 mg (86.3%). C<sub>18</sub>H<sub>12</sub>MnN<sub>10</sub>S<sub>2</sub> (629.24): calcd. C 34.36, H 1.92, N 22.26, S 10.19%; found C 34.31, H 1.90, N 22.22, S 10.21%. IR (ATR):  $\tilde{\nu}_{max} = 3091$  (w), 2099 (w), 2068 (w), 2067 (s), 1577 (w), 1516 (m), 1460 (m), 1380 (m), 1288 (m), 1206 (w), 1137 (m), 1135 (s), 1058 (s), 1016 (s), 917 (m), 844 (s), 812 (s), 766 (m), 734 (m), 635 (m), 489 (s), 435 (m), 409 (s) cm<sup>-1</sup> (see Figure S1, Supporting Information).

**Synthesis of 1-Mn/CH<sub>3</sub>:** Single crystals suitable for X-ray structure determination were obtained by the reaction of Mn(NCS)<sub>2</sub> (25.6 mg, 0.15 mmol) and 2-methylpyrazine (27.4  $\mu$ L, 0.3 mmol) in water (1 mL) in a closed snap cap vial. Yellow block-shaped single crystals were obtained after 3 d at room-temperature. Yield based on Mn(NCS)<sub>2</sub>: 887 mg (74.8%). C<sub>12</sub>H<sub>16</sub>MnN<sub>6</sub>O<sub>2</sub>S<sub>2</sub> (395.36): calcd. C 36.46, H 4.08, N 21.26, S 16.22%; found C 36.51, H 3.98, N 21.47, S 16.18%. IR (ATR):  $\tilde{\nu}_{max} = 3330$  (br), 3167 (br), 2079 (s), 1645 (m), 1519 (m), 1477 (m), 1436 (m), 1406 (m), 1386 (m), 1297 (m), 1161 (w), 1070 (m), 1027 (m), 978 (m), 941 (m), 844 (s), 788 (m), 745 (m), 663 (m), 603 (br), 477 (m), 413 (s) cm<sup>-1</sup> (see Figure S2, Supporting Information).

**Synthesis of 2-Mn/Cl:** Single crystals suitable for X-ray structure determination were obtained by the reaction of Mn(NCS)<sub>2</sub> (25.6 mg, 0.15 mmol) and 2-chloropyrazine (137.0  $\mu$ L, 1.5 mmol) without solvent. Yellow block-shaped single crystals were obtained after 2 d.

**Synthesis of 2-Mn/CH<sub>3</sub>:** Single crystals suitable for X-ray structure determination were obtained by the reaction of Mn(NCS)<sub>2</sub> (25.6 mg, 0.15 mmol) and 2-methylpyrazine (13.7 μL, 0.15 mmol) in ethanol (1 mL) in a closed test-tube at 120 °C. Yellow block-shaped single crystals were obtained on cooling after two weeks.

**Elemental Analysis and IR Data of the Residue obtained in the First TG Step by Thermal Decomposition of 1-Mn/Cl:**

C<sub>10</sub>H<sub>6</sub>MnN<sub>6</sub>S<sub>2</sub> (400.17): calcd. C 30.01, H 1.51, N 21.00, S 16.03%; found C 30.05, H 1.50, N 20.98, S 16.05% **IR** (ATR):  $\tilde{\nu}_{\max}$  = 3076 (w), 2095 (s), 1575 (w), 1516 (m), 1448 (m), 1389 (s), 1284 (w), 1207 (w), 1173 (w), 1136 (s), 1056 (s), 1015 (s), 949 (w), 918 (w), 840 (s), 769 (m), 735 (m), 639 (m), 439 (m), 474 (m), 438 (m), 415 (s) cm<sup>-1</sup> (see Figure S12, Supporting Information).

**Elemental Analysis and IR Data of the Residue obtained in the First TG Step by Thermal Decomposition of 1-Mn/CH<sub>3</sub>:**

C<sub>12</sub>H<sub>12</sub>MnN<sub>6</sub>S<sub>2</sub> (359.33): calcd. C 40.11, H 3.37, N 23.39, S 17.85%; found C 39.63, H 3.34, N 23.25, S 17.93% **IR** (ATR):  $\tilde{\nu}_{\max}$  = 2049 (s), 2034 (s), 1603 (w), 1516 (m), 1482 (m), 1440 (m), 1389 (m), 1304 (m), 1258 (m), 1182 (m), 1152 (m), 1077 (m), 1033 (m), 985 (w), 964 (w), 829 (m), 742 (m), 660 (m), 483 (m), 421 (s) cm<sup>-1</sup> (see Figure S13, Supporting Information).

**Elemental Analysis and IR Data of the Residue obtained in the Second TG Step by Thermal Decomposition of 1-Mn/CH<sub>3</sub>:**

C<sub>7</sub>H<sub>6</sub>MnN<sub>4</sub>S<sub>2</sub> (265.22): calcd. C 31.70, H 2.28, N 21.12, S 24.18%; found C 31.81, H 2.23, N 21.20, S 24.34% **IR** (ATR):  $\tilde{\nu}_{\max}$  = 2099 (s), 2091 (s), 1518 (w), 1485 (m), 1438 (m), 1390 (m), 1302 (m), 1257 (m), 1189 (w), 1159 (m), 1083 (m), 1029 (m), 985 (w), 830 (m), 786

(m), 659 (m), 476 (m), 435 (s) cm<sup>-1</sup> (see Figure S14, Supporting Information).

**Single Crystal Structure Analysis:** Single crystal data collections were carried out with an imaging plate diffraction system (Stoe IPDS-1) with Mo-K<sub>α</sub> radiation. The structures were solved with direct methods using SHELXS-97 and structure refinements were performed against F<sup>2</sup> using SHELXL-97.<sup>[58]</sup> Numerical absorption correction was applied using programs X-RED and X-SHAPE of the program package X-Area.<sup>[59–61]</sup> All non hydrogen atoms were refined with anisotropic displacement parameters. All hydrogen atoms were positioned with idealized geometry and were refined isotropic with U<sub>iso</sub>(H) = -1.2 U<sub>eq</sub>(C) (1.5 for methyl hydrogen atoms) using a riding model. The O–H hydrogen atoms were located in a difference map, their bond lengths were set to ideal values and finally they were refined using a riding model with U<sub>iso</sub>(H) = -1.5 U<sub>eq</sub>(O). The crystal of compound **1-Mn/Cl** is non-merohedrally twinned. Both individuals were indexed separately and from the orientation matrices the twin matrix was calculated (0 0 -1 0 -1 0 -1 0 0). Afterwards symmetry related reflections were merged and a data file in HKLF-5 format was calculated and used in the refinement (BASF: 0.26253). The crystal of **2-Mn/CH<sub>3</sub>** was racemically twinned and therefore, a twin refinement was performed (BASF parameter: 0.2392). Details of the structure determination are given in Table 2.

**X-ray Powder Diffraction (XRPD):** The data collection of **1-Mn/Cl**, **1-Mn/CH<sub>3</sub>**, **3-Mn/CH<sub>3</sub>**, **4-Mn/Cl**, and **4-Mn/CH<sub>3</sub>** were performed with a PANalytical X'Pert Pro MPD reflection powder diffraction system with Cu-K<sub>α</sub> radiation (λ = 0.15406 Å) equipped with a PIXcel semiconductor detector from PANalytical. The data collection of

**Table 2.** Selected crystal data and details on the structure refinements. Please note that the structure of **4-Mn/Cl** and **4-Mn/CH<sub>3</sub>** were determined by Rietveld refinements and the values of the figures of merit are as defined in *TOPAS 4.2*.

	<b>1-Mn/Cl</b>	<b>1-Mn/CH<sub>3</sub></b>	<b>2-Mn/Cl</b>	<b>2-Mn/CH<sub>3</sub></b>	<b>4-Mn/Cl</b>	<b>4-Mn/CH<sub>3</sub></b>
Formula	C <sub>18</sub> H <sub>12</sub> Cl <sub>4</sub> MnN <sub>10</sub> S <sub>2</sub>	C <sub>12</sub> H <sub>16</sub> MnN <sub>6</sub> O <sub>2</sub> S <sub>2</sub>	C <sub>40</sub> H <sub>31</sub> Cl <sub>9</sub> Mn <sub>2</sub> N <sub>22</sub> O <sub>2</sub> S <sub>4</sub>	C <sub>14</sub> H <sub>24</sub> Mn <sub>2</sub> N <sub>8</sub> O <sub>6</sub> S <sub>4</sub>	C <sub>10</sub> H <sub>6</sub> Cl <sub>2</sub> MnN <sub>6</sub> S <sub>2</sub>	C <sub>7</sub> H <sub>6</sub> MnN <sub>4</sub> S <sub>2</sub>
MW /g·mol <sup>-1</sup>	629.24	395.37		638.53	400.17	265.22
Crystal system	monoclinic	triclinic	triclinic	tetragonal	monoclinic	monoclinic
Space group	<i>P</i> 2 <sub>1</sub> / <i>n</i>	<i>P</i> $\bar{1}$	<i>P</i> $\bar{1}$	<i>P</i> 4 <sub>3</sub>	<i>P</i> 2 <sub>1</sub> / <i>c</i>	<i>P</i> 2 <sub>1</sub> / <i>n</i>
<i>a</i> /Å	12.1305(9)	7.004(1)	10.5531(9)	13.545(1)	10.761(25)	8.469(19)
<i>b</i> /Å	7.1695(3)	8.255(1)	11.2649(11)	13.545(1)	9.570(21)	9.433(24)
<i>c</i> /Å	14.639(1)	9.317(1)	12.6071(11)	15.005(2)	15.854(33)	12.867(27)
<i>a</i> /°	90	109.13(2)	85.047(11)	90	90	90
<i>β</i> /°	90.942(9)	111.33(22)	84.632(10)	90	96.92(12)	94.90(12)
<i>γ</i> /°	90	99.32(2)	87.936(11)	90	90	90
<i>V</i> /Å <sup>3</sup>	1273.0(1)	449.2(1)	1486.0(2)	2753.2(3)	1620.82(1)	1024.15(2)
<i>T</i> /K	200	293	200	200	293	293
<i>Z</i>	2	1	1	4	4	4
<i>D</i> <sub>calc</sub> /mg·m <sup>-3</sup>	1.642	1.461	1.575	1.540	1.615	1.612
λ /Å	0.71073	0.71073	0.71073	0.71073	0.7093	1.540596
μ /mm <sup>-1</sup>	1.132	0.983d	1.026	1.263	–	–
θ <sub>max</sub> /°	27.07	27.00	26.00	25.97	38	60
Measured refl.	2729	3881	15111	26326	1365	303
Unique refl.	2729	1900	5709	5390	–	–
<i>R</i> <sub>int</sub>	0.0381	0.0317	0.0313	0.0662	–	–
<i>R</i> <sub>exp</sub>	–	–	–	–	3.689	1.488
<i>R</i> <sub>wp</sub>	–	–	–	–	5.908	2.317
<i>R</i> <sub>p</sub>	–	–	–	–	4.594	1.787
Refl. with <i>F</i> <sub>o</sub> > 4σ( <i>F</i> <sub>o</sub> )	2216	1526	4793	4723	–	–
Parameters	162	108	365	310	70	62
<i>R</i> <sub>1</sub> [ <i>F</i> <sub>o</sub> > 4σ( <i>F</i> <sub>o</sub> )]	0.0420	0.0332	0.0392	0.0370	–	–
<i>wR</i> <sub>2</sub> (all refl.)	0.1413	0.0935	0.1055	0.0925	–	–
GOF	1.115	1.025	1.050	0.997	1.601	1.558
Δρ <sub>max/min</sub> /e·Å <sup>-3</sup>	1.033/–0.450	0.290 / –0.464	1.594 / –1.063	0.313 / –0.391	–	–

**1-Mn/Cl**, **1-Mn/CH<sub>3</sub>**, **3-Mn/CH<sub>3</sub>**, **4-Mn/Cl**, and **4-Mn/CH<sub>3</sub>** were performed by Stoe transmission powder diffraction system (STADI-P) with Cu-K $\alpha$  radiation ( $\lambda = 154.0598$  pm) that was equipped with a linear position-sensitive detector from STOE & CIE. The data collection of **4-Mn/Cl** was performed with a high-resolution powder diffractometer Bruker D8 Advance with Ge(111)-Johanson-type monochromator and VÅNTEC-1 position sensitive detector in Debye-Scherrer geometry.

**Rietveld Refinements:** Rietveld refinement<sup>[60]</sup> was performed using the program TOPAS 4.2.<sup>[61]</sup> Selected crystallographic data are listed in Table 2. The refined overall parameters were: phase scale factor, background coefficients (Chebyshev polynomials), unit cell parameters, zero-error shift, and parameters for the strain contribution. The anisotropy of width and asymmetry of the Bragg reflections was successfully modeled by applying symmetry adapted spherical harmonics of eight's order to Gaussian, Lorentzian, and exponential distributions, which are then convoluted with geometrical and instrumental contributions to the final peak profile.

Crystallographic data (excluding structure factors) for the structures in this paper have been deposited with the Cambridge Crystallographic Data Centre, CCDC, 12 Union Road, Cambridge CB21EZ, UK. Copies of the data can be obtained free of charge on quoting the depository numbers CCDC-957591 (**1-Mn/CH<sub>3</sub>**), -957592 (**1-Mn/Cl**), -957593 (**2-Mn/CH<sub>3</sub>**), -957594 (**2-Mn/Cl**), -957595 (**4-Mn/CH<sub>3</sub>**) and -957596 (**4-Mn/Cl**) (Fax: +44-1223-336-033; E-Mail: deposit@ccdc.cam.ac.uk, http://www.ccdc.cam.ac.uk).

**Elemental Analysis:** CHNS analysis was performed with an EURO EA elemental analyzer, fabricates by EURO VECTOR Instruments and Software.

**Differential Thermal Analysis and Thermogravimetry (DTA-TG):** These measurements were performed in a nitrogen atmosphere (purity: 5.0) in Al<sub>2</sub>O<sub>3</sub> crucibles with a STA-409CD thermobalance from Netzsch. The instrument was calibrated using standard references materials. All measurements were performed with a heating rate of 4 K·min<sup>-1</sup> and a low rate of 75 mL·min<sup>-1</sup>.

**Magnetic Measurements:** All magnetic measurements were performed with a PPMS (Physical Property Measurement System) from Quantum Design, which was equipped with a 9 Tesla magnet. The data were corrected for core diamagnetism.

**Supporting Information** (see footnote on the first page of this article): IR spectra for compounds **1-Mn/Cl**, **1-Mn/CH<sub>3</sub>**, **3-Mn/Cl**, **4-Mn/Cl**, **3-Mn/CH<sub>3</sub>**, **4-Mn/CH<sub>3</sub>**, ORTEP plots of **1-Mn/Cl**, **1-Mn/CH<sub>3</sub>**, **2-Mn/CH<sub>3</sub>**, **2-Mn/Cl**, experimental XRPD pattern of the residue in the first heating step of **1-Mn/CH<sub>3</sub>**. Crystal structures of **4-Mn/Cl**, **4-Mn/CH<sub>3</sub>**, magnetic measurements of **1-Mn/Cl**, **1-Mn/CH<sub>3</sub>**, **3-Mn/CH<sub>3</sub>**, **4-Mn/Cl**, **4-Mn/CH<sub>3</sub>**.

## Acknowledgements

This project was supported by the Deutsche Forschungsgemeinschaft (Project No. Na 720/3-1) and the State of Schleswig-Holstein. We thank Prof. Dr. Wolfgang Bensch for access to his experimental facilities. Special thanks to Inke Jess for the single crystal measurements and Maren Rasmussen as well as Henning Lühmann for the magnetic measurements.

## References

[1] X.-Y. Wang, Z.-M. Wang, S. Gao, *Chem. Commun.* **2008**, 281.

- [2] E. Pardo, R. Ruiz-Garcia, J. Cano, X. Ottenwaelder, R. Lescouezec, Y. Journaux, F. Lloret, M. Julve, *Dalton Trans.* **2008**, 2780.
- [3] A. Y. Robin, K. M. Fromm, *Coord. Chem. Rev.* **2006**, 250, 2127.
- [4] D. MasPOCH, D. Ruiz-Molina, J. Veciana, *J. Mater. Chem.* **2004**, 14, 2713.
- [5] C. Janiak, *Dalton Trans.* **2003**, 2781.
- [6] D. Braga, L. Maini, M. Polito, L. Scaccianocce, G. Cozzani, F. Grepioni, *Coord. Chem. Rev.* **2001**, 216, 225.
- [7] C. Janiak, J. K. Vieth, *New J. Chem.* **2010**, 34, 2366.
- [8] K. S. Gavrilenko, O. Cador, K. Bernot, P. Rosa, R. Sessoli, S. Golhen, V. V. Pavlishchuk, L. Ouahab, *Chem. Eur. J.* **2008**, 14, 2034.
- [9] X.-Y. Wang, H.-Y. Wei, Z.-M. Wang, Z.-D. Chen, S. Gao, *Inorg. Chem.* **2005**, 44, 572.
- [10] J. Ferrando-Soria, R. Ruiz-García, J. Cano, S.-E. Stiriba, J. Vallejo, I. Castro, M. Julve, F. Lloret, P. Amorós, J. Pasán, C. Ruiz-Pérez, Y. Journaux, E. Pardo, *Chem. Eur. J.* **2012**, 18, 1608.
- [11] Y.-F. Zeng, X. Hu, F.-C. Liu, X.-H. Bu, *Chem. Soc. Rev.* **2009**, 38, 469.
- [12] R. Vicente, B. Bitschnau, A. Egger, B. Sodin, F. A. Mautner, *Dalton Trans.* **2009**, 5120.
- [13] E.-C. Yang, Z.-Y. Liu, T.-Y. Liu, L.-L. Li, X.-J. Zhao, *Dalton Trans.* **2011**, 40, 8132.
- [14] C. J. Adams, M. C. Muñoz, R. E. Waddington, J. A. Real, *Inorg. Chem.* **2011**, 50, 10633.
- [15] C. J. Adams, M. F. Haddow, D. J. Harding, T. J. Podesta, R. E. Waddington, *CrystEngComm* **2011**, 13, 4909.
- [16] C. J. Adams, J. A. Real, R. E. Waddington, *CrystEngComm* **2010**, 12, 3547.
- [17] J.-Q. Tao, Z.-G. Gu, T.-W. Wang, Q.-F. Yang, J.-L. Zuo, X.-Z. You, *Inorg. Chim. Acta* **2007**, 360, 4125.
- [18] J. M. Shi, J. N. Chen, C. J. Wu, J. P. Ma, *J. Coord. Chem.* **2007**, 60, 2009.
- [19] T. K. Maji, G. Mostafa, J. M. Clemente-Juan, J. Ribas, F. Lloret, K.-I. Okamoto, N. R. Chaudhuri, *Eur. J. Inorg. Chem.* **2003**, 1005.
- [20] F. Lloret, M. Julve, J. Cano, G. D. Munno, *Mol. Cryst. Liq. Cryst.* **1999**, 334, 569.
- [21] F. Lloret, G. De Munno, M. Julve, J. Cano, R. Ruiz, A. Caneschi, *Angew. Chem. Int. Ed.* **1998**, 37, 135.
- [22] E. Shurdha, S. H. Lapidus, P. W. Stephens, C. E. Moore, A. L. Rheingold, J. S. Miller, *Inorg. Chem.* **2012**, 51, 9655.
- [23] S. Han, S.-L. Dai, W.-Q. Chen, J.-R. Zhou, L.-M. Yang, C.-L. Ni, *J. Coord. Chem.* **2012**, 65, 2751.
- [24] J.-F. Létard, C. Carbonera, J. A. Real, S. Kawata, S. Kaizaki, *Chem. Eur. J.* **2009**, 15, 4146.
- [25] T. Yi, C. Ho-Chol, S. Gao, S. Kitagawa, *Eur. J. Inorg. Chem.* **2006**, 2006, 1381.
- [26] M. Wriedt, I. Jeß, C. Näther, *Eur. J. Inorg. Chem.* **2009**, 1406.
- [27] M. Wriedt, S. Sellmer, C. Näther, *Inorg. Chem.* **2009**, 48, 6896.
- [28] M. Wriedt, S. Sellmer, C. Näther, *Dalton Trans.* **2009**, 7975.
- [29] M. Wriedt, C. Näther, *Eur. J. Inorg. Chem.* **2010**, 3201.
- [30] S. Wöhlert, M. Wriedt, T. Fic, Z. Tomkowicz, W. Haase, C. Näther, *Inorg. Chem.* **2013**, 52, 1061.
- [31] M. Wriedt, C. Näther, *Z. Anorg. Allg. Chem.* **2010**, 636, 569.
- [32] C. Näther, J. Greve, *J. Solid State Chem.* **2003**, 176, 259.
- [33] M. Wriedt, C. Näther, *Chem. Commun.* **2010**, 46, 4707.
- [34] S. L. James, C. J. Adams, C. Bolm, D. Braga, P. Collier, T. Friscic, F. Grepioni, K. D. M. Harris, G. Hyett, W. Jones, A. Krebs, J. Mack, L. Maini, A. G. Orpen, I. P. Parkin, W. C. Shearouse, J. W. Steed, D. C. Waddell, *Chem. Soc. Rev.* **2012**, 41, 413.
- [35] C. J. Adams, M. A. Kurawa, M. Lusi, A. G. Orpen, *CrystEngComm* **2008**, 10, 1790.
- [36] D. Braga, S. L. Giaffreda, F. Grepioni, A. Pettersen, L. Maini, M. Curzi, M. Polito, *Dalton Trans.* **2006**, 1249.
- [37] K. Müller-Buschbaum, *Z. Anorg. Allg. Chem.* **2005**, 631, 811.
- [38] J. Boeckmann, C. Näther, *Dalton Trans.* **2010**, 39, 11019.
- [39] J. Boeckmann, C. Näther, *Chem. Commun.* **2011**, 47, 7104.
- [40] J. Boeckmann, M. Wriedt, C. Näther, *Chem. Eur. J.* **2012**, 18, 5284.

- [41] S. Wöhlert, U. Ruschewitz, C. Näther, *Cryst. Growth Des.* **2012**, *12*, 2715.
- [42] S. Wöhlert, J. Boeckmann, M. Wriedt, C. Näther, *Angew. Chem. Int. Ed.* **2011**, *50*, 6920.
- [43] H.-L. Sun, Z.-M. Wang, S. Gao, *Coord. Chem. Rev.* **2010**, *254*, 1081.
- [44] W.-X. Zhang, R. Ishikawa, B. Breedlovea, M. Yamashita, *RSC Adv.* **2013**, *3*, 3772.
- [45] H. Miyasaka, R. Clérac, *Bull. Chem. Soc. Jpn.* **2005**, *78*, 1725.
- [46] C. Coulon, H. Miyasaka, R. Clérac, *Struct. Bonding (Berlin)* **2006**, *122*, 163.
- [47] A. Caneschi, D. Gatteschi, N. Lalioti, C. Sangregorio, R. Sessoli, G. Venturi, A. Vindigni, A. Rettori, M. G. Pini, M. A. Novak, *Angew. Chem. Int. Ed.* **2001**, *40*, 1760.
- [48] J. Boeckmann, C. Näther, *Polyhedron* **2012**, *31*, 587.
- [49] S. Wöhlert, L. Fink, M. Schmidt, C. Näther, *Z. Anorg. Allg. Chem.* **2013**, in press, doi: 10.1002/zaac.201300222.
- [50] S. Wöhlert, I. Jess, C. Näther, *Z. Naturforsch. B* **2012**, *67*, 41.
- [51] S. Wöhlert, L. Peters, C. Näther, *Dalton Trans.* **2013**, *42*, 10746.
- [52] S. Wöhlert, C. Näther, *Inorg. Chim. Acta* **2013**, *406*, 196.
- [53] S. Wöhlert, C. Näther, *Eur. J. Inorg. Chem.* **2013**, *2013*, 2528.
- [54] S. Wöhlert, L. Fink, M. Schmidt, C. Näther, *CrystEngComm* **2013**, *15*, 945.
- [55] I. Jeß, J. Boeckmann, C. Näther, *Dalton Trans.* **2012**, *41*, 228.
- [56] J. Boeckmann, I. Jeß, T. Reinert, C. Näther, *Eur. J. Inorg. Chem.* **2011**, 5502.
- [57] S. Wöhlert, C. Näther, *Z. Anorg. Allg. Chem.* **2012**, *638*, 2265.
- [58] G. M. Sheldrick, *Acta Crystallogr. Sect. A* **2008**, *64*, 112.
- [59] *X-Red*, Version 1.11, Program for Data Reduction and Absorption Correction, STOE & CIE GmbH, Darmstadt, Germany, **1998**.
- [60] *X-Shape*, Version 1.03, Program for the Crystal Optimization for Numerical Absorption Correction, STOE & CIE GmbH, Darmstadt, Germany, **1998**.
- [61] *X-Area*, Version 1.44, Program Package for Single Crystal Measurements, STOE & CIE GmbH, Darmstadt, Germany, **2008**.

Received: July 22, 2013

Published Online: September 20, 2013